Macromolecular
Rapid Communication
www.mrc-journal.d

Ionic Strength and Thermal Dual-Responsive Bilayer Hollow Spherical Hydrogel Actuator

Shengzhu Zhou, Baoyi Wu, Qiang Zhou, Yukun Jian, Xiaoxia Le, Huanhuan Lu, Dachuan Zhang, Jiawei Zhang, Zhihui Zhang,* and Tao Chen*

As one of the most promising intelligent materials, polymeric hydrogel actuators could produce reversible shape change upon external stimuli. Although complex shape deformation from 2D to 3D have been achieved, the realization of actuating behavior from 3D to 3D is still a significant challenge. Herein, an effective strategy to develop a novel bilayer hollow spherical hydrogel actuator is proposed. Through immersing a Ca^{2+} incorporated gelatin core into alginate solution, an ionic-strength-responsive alginate layer will be formed along the gelatin core via alginate–Ca^{2+} crosslinks, and then another thermo-responsive alginate-poly(2-(dimethylamino) ethyl methacrylate)(Alg-PDMAEMA) layer is introduced to achieve a bilayer hydrogel with ionic strength and temperature dual responsiveness. A hollow hydrogel capsule could be obtained if a spherical gelatin core is applied, and it could produce complex shape deformations from 3D to 3D upon the trigger of ionic strength and temperatures changes. The present work may offer new inspirations for the development of novel intelligent polymeric hydrogel actuators.

Nature has provided enormous inspirations for the developing of novel intelligent materials that can adapt and actuate upon external stimuli.[1–5] In particular, polymeric hydrogel actuators have the ability to generate reversible shape deformation in response to certain stimuli,[6,7] and in addition to their soft and wet nature similar to living creatures, they have arousing increasing interest and show promising applications as biomimetic actuators,[8–11] soft robots,[12,13] sensors,[14,15] and so on. In the beginning, the investigated hydrogel actuators could only produce simple swelling/shrinking because of the isotropic structures.[16,17] In the current stage, complex shape transformations could be realized by fabricating anisotropic structures or using uneven stimulus.[18–22] However, most of the reported hydrogel actuators only provide complex deformations from 2D to 3D, because the initial shape of the hydrogel actuators are restricted by mold, even with 3D printing, planar hydrogel actuators are usually fabricated which is probably due to the soft and wet nature.[23–28] While in nature, the living organisms have 3D structures, and most of the deformations/movements are from 3D to 3D. In order to expand the potential applications of hydrogel actuators, it is significantly important to explore hydrogels that could generate complex deformations from 3D to 3D upon external stimuli. A few efforts have been devoted to construct hydrogel actuators with 3D initial shapes.[29–31] For instance, Zhou and co-workers have prepared symmetric/asymmetric hollow hydrogel tubes as thermo-responsive actuators through surface catalytically initiated radical polymerization approach.[31] In our previous work, we have also designed 3D hydrogel actuators through fabricating a patterned second network or glue a collapsed thermo-responsive actuating layer with a passive layer to realize complex 3D shape transformations.[18,32]

Herein, we present a novel bilayer hollow spherical hydrogel actuator with ionic strength and thermal dual responsiveness. First of all, a gelatin hydrogel with Ca^{2+} was immersed into the solution of alginate to induce the formation of an alginate layer through metal coordination between alginate chains and Ca^{2+}, then a second double network alginate-poly(2-(dimethylamino) ethyl methacrylate)(Alg-PDMAEMA) layer was introduced by initiating the polymerization of DMAEMA monomers as the formation of alginate network, and a bilayer hydrogel could

---

S. Zhou, Q. Zhou, Prof. Z. Zhang
Key Laboratory of Bionic Engineering (Ministry of Education) and
College of Biological and Agricultural Engineering
Jilin University
Changchun 130022, China
E-mail: zhzh@jlu.edu.cn

S. Zhou
Department of Anesthesiology
The Second Hospital of Jilin University
Changchun 130061, China

B. Wu, Y. Jian, Dr. X. Le, H. Lu, D. Zhang, Prof. J. Zhang, Prof. T. Chen
Key Laboratory of Marine Materials and Related Technologies
Zhejiang Key Laboratory of Marine Materials
and Protective Technologies
Ningbo Institute of Material Technology and Engineering
Chinese Academy of Sciences
Ningbo 315201, China
E-mail: zhangjiawei@nimte.ac.cn

Q. Zhou
Cadre's Ward
The First Hospital of Jilin University
Changchun 130021, China

The ORCID identification number(s) for the author(s) of this article can be found under https://doi.org/10.1002/marc.201900543.

DOI: 10.1002/marc.201900543

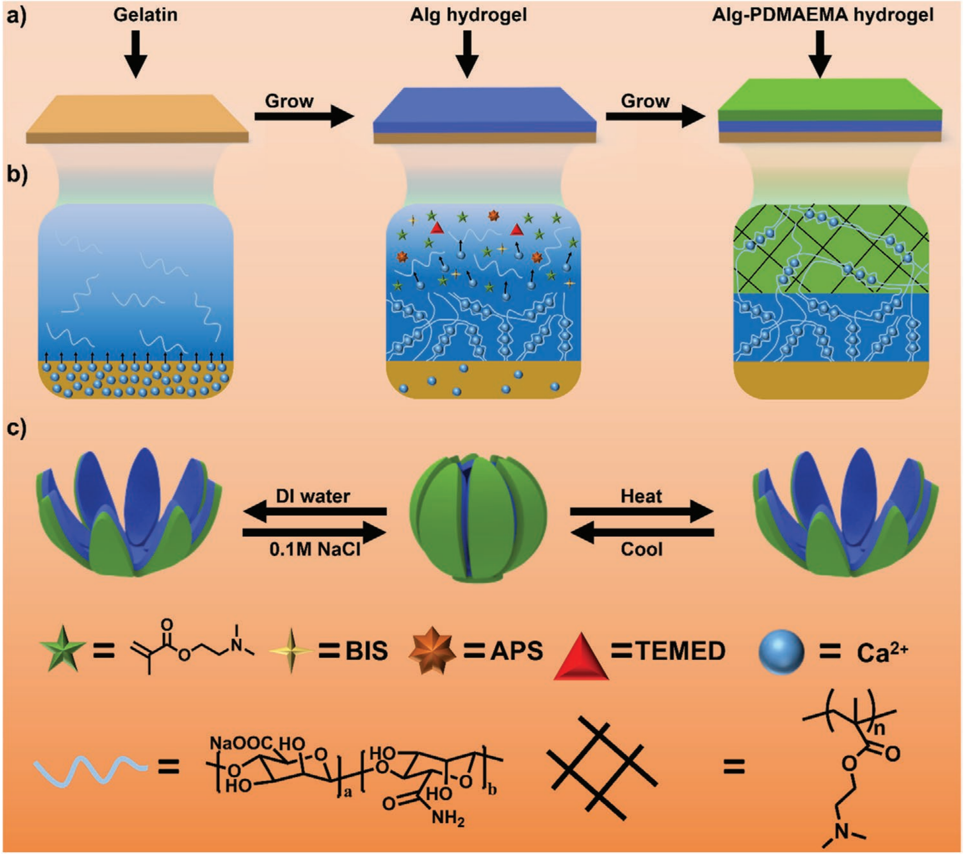

Scheme 1. a) Schematic illustration of the fabrication of asymmetric bilayer hydrogel. A gelatin hydrogel containing Ca^{2+} is immersed into the solution of alginate, an alginate layer will be generated caused by the diffusion-induced gelation, then another Alg-PDMAEMA layer will be formed. b) Schematic illustration of the pH and ionic strength dual-responsive hollow spherical hydrogel actuator.

be obtained by removing the gelatin hydrogel (**Scheme 1**a,b). The obtained bilayer hydrogel could produce shape deformations upon the trigger of ionic strength and temperature, and complex actuating behavior could be accomplished by creating a patterned second layer. Moreover, hollow hydrogel capsules which could generate complex shape deformations from 3D to 3D have been prepared (Scheme 1c). We have presented an effective strategy to accomplish actuating performance from 3D to 3D, which may inspire the development of novel stimuli-responsive hydrogels.

The alginate hydrogel was fabricated by diffusion-induced gelation. First of all, a gelatin hydrogel sheet containing $CaCl_2$ was immersed into the solution of alginate, and an alginate layer will be formed on the top of the gelatin layer because Ca^{2+} would diffuse from the gelatin layer and crosslink the alginate chains. The thickness of the alginate layer is related to the growth time (**Figure 1**a), as the time increases from 0.5 to 3 h, the thickness of the alginate layer increases from ≈0.5 to ≈1.9 mm, simultaneously. Moreover, the thickness of the alginate layer is also dependent on the concentration of Ca^{2+}. If there are more Ca^{2+} in the gelatin layer, more Ca^{2+} will diffuse into the alginate solution, and more alginate-Ca^{2+} crosslinks will be formed, the thickness of the alginate layer will increase as a result (Figure 1c). Not only the thickness, but also the stiffness of the alginate layer can be tuned by the concentration of Ca^{2+}. As shown in **Figure 2**c, both the storage modulus (G') and loss modulus (G'') increase with increasing concentration of Ca^{2+}, which further indicates more alginate-Ca^{2+} are formed with higher concentration of Ca^{2+}. The microstructures of the alginate layer was investigated by scanning electronic microscopy (SEM), as shown in Figure 2e, the alginate layer shows a typical porous structure.

Since the responsiveness of the alginate layer is limited, in order to achieve complex shape deformations under external stimuli, a thermo-responsive PDMAEMA network was introduced. The as-prepared alginate hydrogel was transferred to alginate solution with DMAEMA monomers, *N,N'*-methylenebisacrylamide (BIS) as crosslinker, ammonium peroxodisulfate (APS) as initiator, and *N,N,N',N'*-tetramethylethylenediamine (TEMED) as accelerator. As alginate chains is crosslinked by Ca^{2+}, PDMAEMA network will be formed simultaneously since TEMED promotes the decomposition of the initiator and initiates the polymerization of DMAEMA monomers, and a second alginate-PDMAEMA network will be formed. After peeling off the gelatin hydrogel, a bilayer hydrogel with alginate hydrogel as one layer and interpenetrating alginate-PDMAEMA network as another will be obtained. The bilayer structure was investigated by SEM, as shown in Figure 2a, the alginate and alginate-PDMAMA network exhibit similar porous microstructures, and a clear boundary could be observed between the two layers.

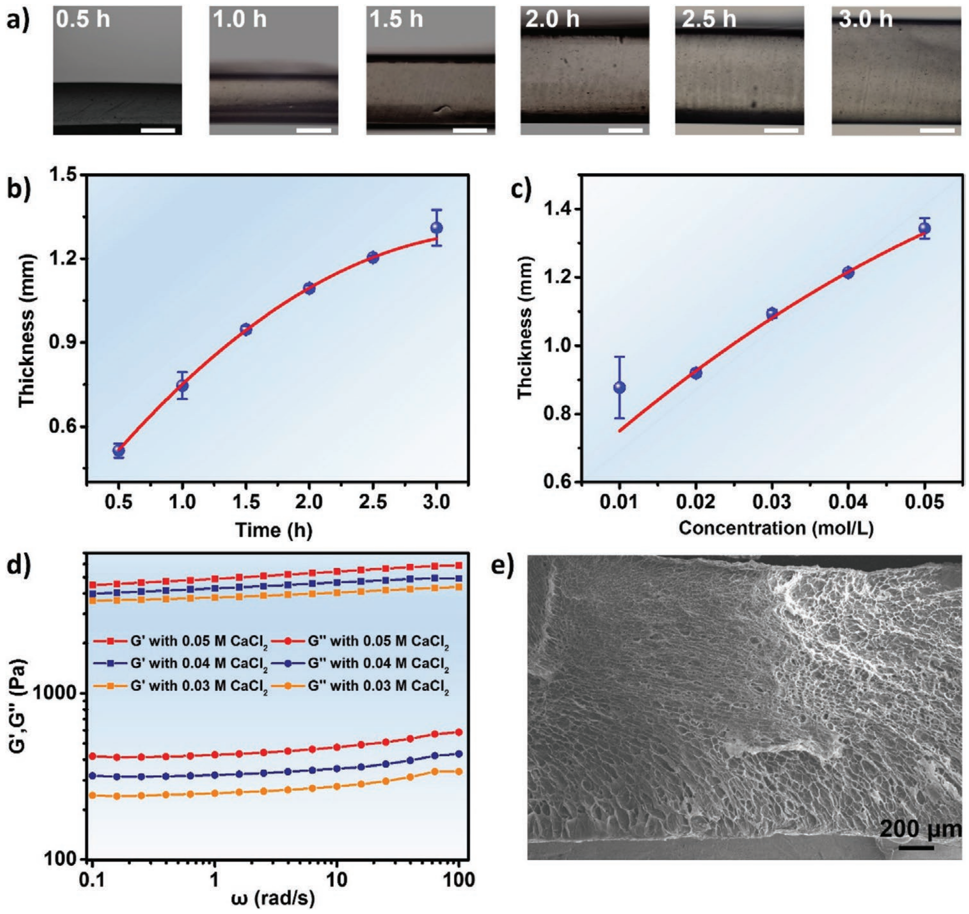

Figure 1. a) Optical images showing hydrogel growth process (Scale bar: 0.5 mm). b) The dependence of the hydrogel thickness as a function of growth time. c) The dependence of the hydrogel thickness as a function of the concentration of alginate (growth time: 2 h). d) Storage modulus G' and loss modulus G'' of hydrogel with different concentration of $CaCl_2$. e) SEM image of the freeze-dried hydrogel.

Since there are large amount of negative charges on the alginate network, the alginate layer would swell in deionized water, while it is almost not swell in NaCl solution (0.1 M), because the electrostatic repulsion between the alginate chains can be depressed by NaCl (Figure S1, Supporting Information). With the introduction of PDMAEMA network, the negative charges and positive charges of the Alg-PDMAEMA layer will be shielded by each other, and the Alg-PDMAEMA network would not swell in both deionized water and NaCl solution. Therefore, the Alg/Alg-PDMAEMA bilayer hydrogel would bend toward the alginate-PDMAEMA layer if it is immersed into deionized water, and it would unbend when it is transferred to 0.1 M NaCl solution. The bending performance is related to the thickness of the two layers. As shown in Figure 2b, the alginate layer is the actuating layer in the shape deforming process, and a thin alginate layer is benefit the actuating performance.

Because of the thermo-responsiveness of the PDMAEMA network, the bilayer hydrogel could produce shape deformation upon the changing of temperature. The swelling properties of each layer in cold and warm water have been investigated. As shown in Figure S2a (Supporting Information), whether in cold (10 °C) or warm (60 °C) environment, the alginate layer would swell. While the Alg-PDMAEMA layer would swell in cold water, and shrink in warm milieu due to the thermal transition of the PDMAEMA network. As shown in Figure 2c, when the bilayer hydrogel was immersed into warm water (60 °C, 0.1 M NaCl), the PDMAEMA network would shrink, and the bilayer hydrogel would bend to the side with PDMAEMA. If the hydrogel was then transferred to cold water (10 °C, 0.1 M NaCl), the PDMAEMA network would swell, and the bilayer hydrogel would unfold. In this shape deformation process, the Alg-PDMAEMA layer is the actuating layer, and a thick Alg-PDMAEMA layer will benefit the deforming process. When the ratio of the alginate layer and Alg-PDMAEMA layer reaches 1:2, the hydrogel achieves a highest bending angle, and it will recover to the original state in cold water (10 °C, 0.1 M NaCl). When both of the two layers are 1 mm, the hydrogel accomplish a medium bending state. Since the shrinking degree of the Alg-PDMAEMA layer is related to temperature (Figure S2b, Supporting Information), the bending performance of the bilayer hydrogel is also influenced by temperature, and the bending angle is increased with increasing temperature (Figure 2d).

Besides simple shape deformation from strip to circle, complex shape deformation could be obtained by patterning design of the thermo-responsive Alg-PDMAEMA layer. As shown in **Figure 3**a, a planar hydrogel sheet with a 45° diagonal patterned Alg-PDMAEMA layer would deform when the temperature of

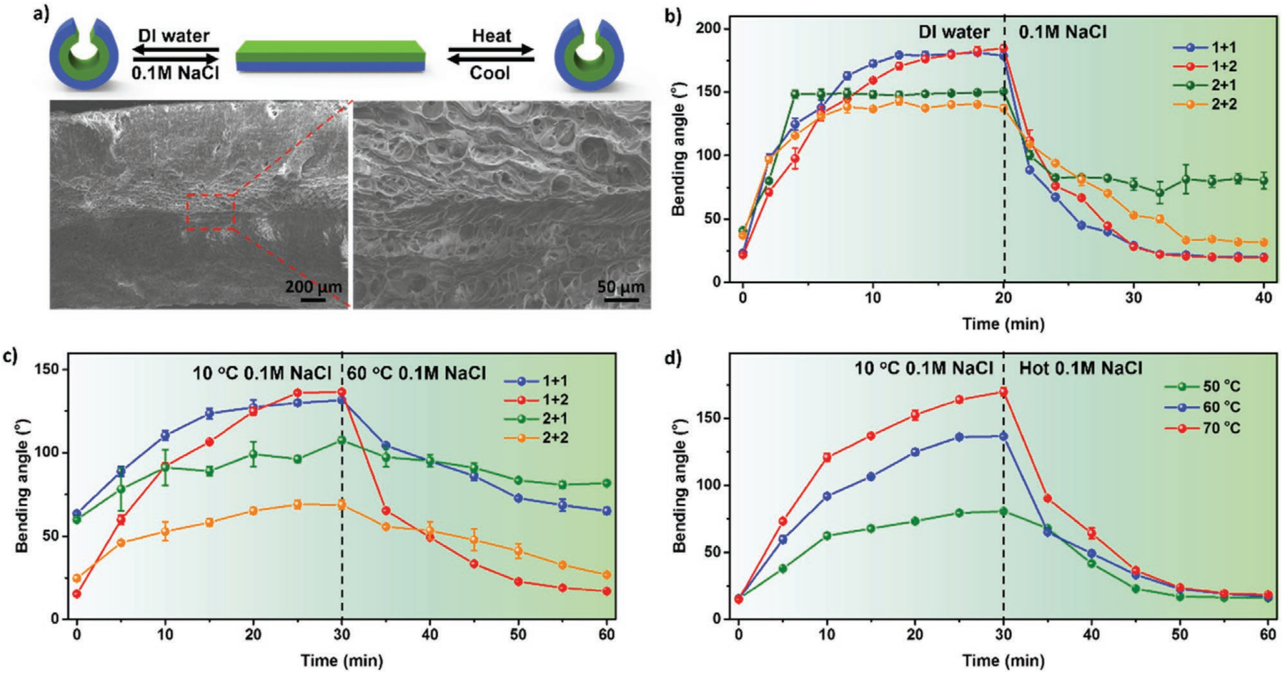

Figure 2. a) Illustration showing the ionic strength and thermal actuating performance of the bilayer hydrogel; Cross section SEM image of a bilayer hydrogel. b) The reversible ionic-strength-induced actuating process of the bilayer hydrogels with different thickness. c) The reversible thermal-induced actuating process of the bilayer hydrogels with different thickness. d) The reversible actuating process of the bilayer hydrogels in different temperatures.

the environment is increased from 10 to 60 °C, and it could further actuate into a cylinder if the concentration of NaCl is decreased from 0.1 M to zero. By deliberately designing the pattern (Figure S3, Supporting Information), a hydrogel triangle would deform to a cigar-like cylinders (Figure 3b), a hydrogel disc would turn into a saddle (Figure 3c), a flat hydrogel leaf would curl (Figure 3d), and a hydrogel flower would close (Figure 3e). In general, with predesigned pattern, complex shape transformation from 2D to 3D could occur by tuning the temperature and ionic strength step by step, and

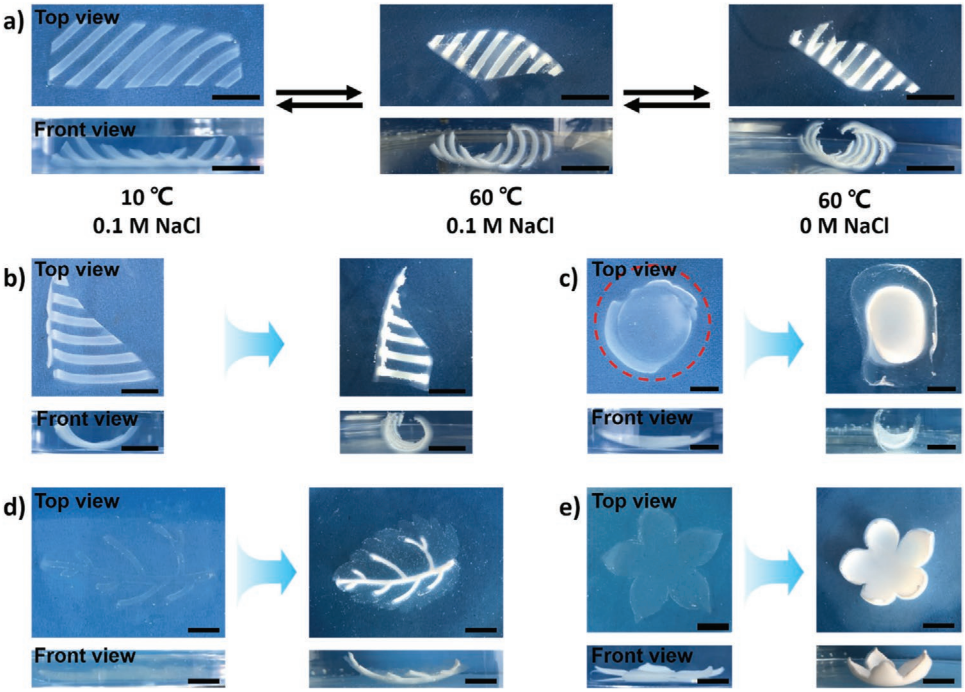

Figure 3. a) The thermo- and ionic-strength-responsive actuating process of a planar hydrogel sheet with patterned Alg-PDMAEMA layer. The actuating process of hydrogel b) triangle, c) circle, d) leaf, and e) flower with patterned Alg-PDMAEMA layer. (Scale bar: 1 cm)

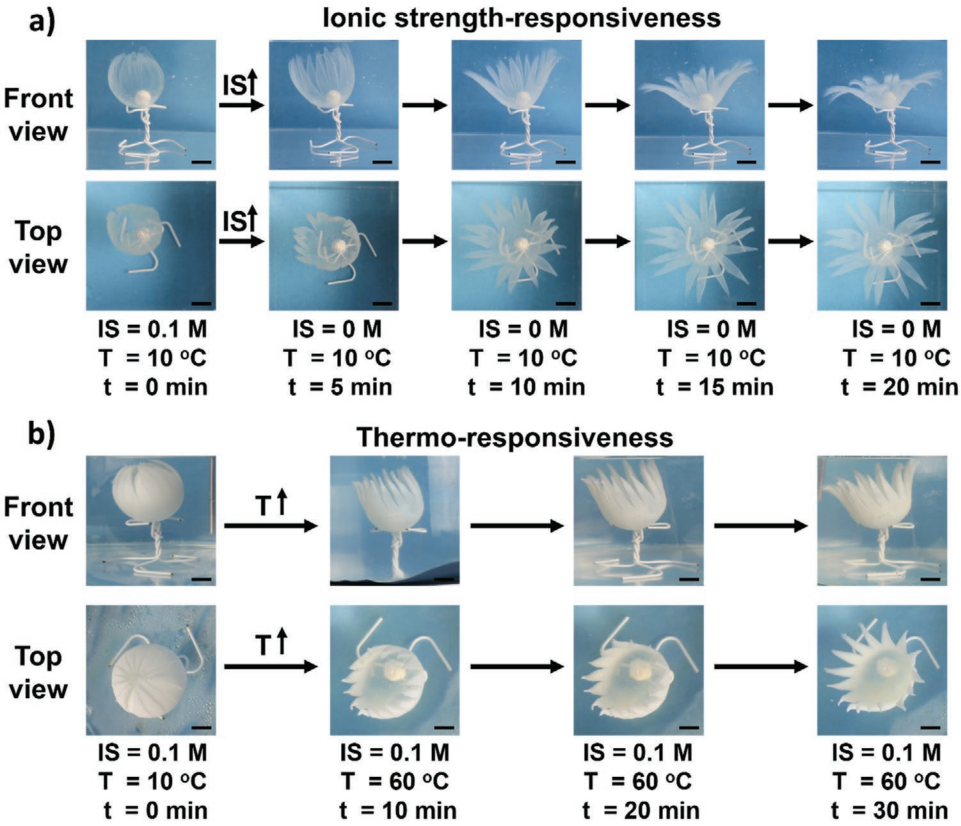

Figure 4. The ionic strength and thermo-responsive shape deformation process of hollow hydrogel capsules. a) A hollow hydrogel sphere would open if it is transferred from 0.1 M NaCl solution to deionized water due to the swell of the inner alginate layer. b) A hollow hydrogel sphere would unfold in 60 °C aqueous solution because of the shrink of the outer Alg-PDMAEMA layer. (Scale bar: 1 cm)

a more complicated actuating behavior could be expected through this strategy.

The remarkable actuating process of the bilayer hydrogel encourages us to explore the deformation of a more complex structure. A spherical bilayer hydrogel was fabricated through using a sphere shaped gelatin hydrogel, then the hydrogel was cut open, and the gelatin core was removed to achieve a hollow hydrogel sphere with an inner alginate layer and an outer Alg-PDMAEMA layer (Figure S4, Supporting Information). The hollow hydrogel sphere shows ionic strength and thermo-responsiveness as expected. As shown in **Figure 4**a, if a hollow hydrogel sphere is transferred from 0.1 M NaCl aqueous solution to deionized water, the inner alginate layer would swell, and the hollow hydrogel would open the petals. In addition, after a change of temperature from 10 to 60 °C, the outer Alg-PDMAEMA layer would shrink, and the hydrogel capsule would unfold as a result (Figure 4b). Both the ionic strength and thermo-responsive shape deformation are reversible (Figure S5, Supporting Information). These hydrogel capsules with programmable shape transformation may have potential application as drug carriers, and the wrapped drugs could be released during the actuating process in response to ionic strength and temperature changes.

In conclusion, we have presented a novel ionic strength and thermo-responsive bilayer hydrogel actuator. The first ionic strength-responsive alginate layer was fabricated by coordination between alginate chains and Ca^{2+} diffused from gelatin, then a second thermo-responsive Alg-PDMAEMA layer was introduced by diffusion induced gelation with simultaneously polymerization of DMAEMA, realizing ionic strength and thermal dual responsive actuating behaviors. Moreover, 3D complex shape deformations could be achieved through constructing a patterned Alg-PDMAEMA layer. In addition, hollow hydrogel capsules could be obtained by starting with a spherical gelatin core, and the hollow hydrogel capsules could unfold in response to ionic strength and temperature changes, render the hollow hydrogel capsules potential candidates in drug release field. We believe the present work would contribute to the design and fabrication of novel intelligent materials with promising applications.

Supporting Information

Supporting Information is available from the Wiley Online Library or from the author.

Acknowledgements

S.Z. and B.W. contributed equally to this work. This work was supported by the National Key Research and Development Program of China

(2018YFB1105100), National Natural Science Foundation of China (51873223, 51773215, 21774138), Key Research Program of Frontier Science, Chinese Academy of Sciences (QYZDB-SSW-SLH036), the Natural Science Foundation of Ningbo (2018A610035), Youth Innovation Promotion Association of Chinese Academy of Sciences (2017337, 2019297).

Conflict of Interest

The authors declare no conflict of interest.

Keywords

hydrogel actuators, hydrogel capsules, intelligent materials, ionic strength, shape deformation

Received: October 12, 2019
Revised: December 24, 2019

---

[1] R. Kempaiah, Z. H. Nie, *J. Mater. Chem. B* **2014**, *2*, 2357.
[2] Z. G. Zhao, R. C. Fang, Q. F. Rong, M. J. Liu, *Adv. Mater.* **2017**, *29*, 1703045.
[3] T. Mastuda, R. Kawakami, R. Namba, T. Nakajinma, J. P. Gong, *Science* **2019**, *363*, 504.
[4] P. Rao, T. L. Sun, L. Chen, R. Takahashi, G. Shinohara, H. Guo, D. R. King, T. Kurokawa, J. P. Gong, *Adv. Mater.* **2018**, *30*, 1801884.
[5] D. L. Gan, W. S. Xing, L. L. Jiang, J. Fang, C. C. Zhao, F. Z. Ren, L. M. Fang, K. F. Wang, X. Lu, *Nat. Commun.* **2019**, *10*, 1487.
[6] X. Z. Yan, F. Wang, B. Zheng, F. H. Huang, *Chem. Soc. Rev.* **2012**, *41*, 6042.
[7] H. Ko, A. Javey, *Acc. Chem. Res.* **2017**, *50*, 691.
[8] L. Zhao, J. H. Huang, Y. C. Zhang, T. Wang, W. X. Sun, Z. Tong, *ACS Appl. Mater. Interfaces* **2017**, *9*, 11866.
[9] X. Li, X. B. Cai, Y. F. Gao, M. J. Serpe, *J. Mater. Chem. B* **2017**, *5*, 2804.
[10] E. Wang, M. S. Desai, S. W. Lee, *Nano Lett.* **2013**, *13*, 2826.
[11] C. Yao, Z. Liu, C. Yang, W. Wang, X. J. Ju, R. Xie, L. Y. Chu, *Adv. Funct. Mater.* **2015**, *25*, 2980.
[12] D. Han, C. Farino, C. Farino, C. Yang, T. Scott, D. Browe, W. Choi, J. W. Freeman, H. Lee, *ACS Appl. Mater. Interfaces* **2018**, *10*, 17512.
[13] S. J. Kim, O. Kim, M. J. Park, *Adv. Mater.* **2018**, *30*, 1706547.
[14] M. H. Liao, P. B. Wan, J. R. Wen, M. Gong, X. X. Wu, Y. G. Wang, R. Shi, L. Q. Zhang, *Adv. Funct. Mater.* **2017**, *27*, 1703852.
[15] T. J. Long, Y. X. Li, X. Fang, J. Q. Sun, *Adv. Funct. Mater.* **2018**, *28*, 1804416.
[16] S. J. Kim, M. S. Kim, S. I. Kim, G. M. Spinks, B. C. Kim, G. G. Wallace, *Chem. Mater.* **2006**, *18*, 5805.
[17] L. Ionov, *Adv. Funct. Mater.* **2013**, *23*, 4555.
[18] C. X. Ma, X. X. Le, X. L. Tang, J. He, P. Xiao, J. Zheng, H. Xiao, W. Lu, J. W. Zhang, Y. J. Huang, T. Chen, *Adv. Funct. Mater.* **2016**, *26*, 8670.
[19] Z. L. Wu, M. Moshe, J. Grener, H. T. Aubin, Z. H. Nie, E. Sharon, E. Kumacheva, *Nat. Commun.* **2013**, *4*, 1586.
[20] R. C. Luo, J. Wu, N. D. Dinh, C. H. Chen, *Adv. Funct. Mater.* **2015**, *25*, 7272.
[21] S. W. Xiao, M. Z. Zhang, X. M. He, L. Huang, Y. X. Zhang, B. P. Ren, M. Q. Zhong, Y. Chang, J. T. Yang, J. Zheng, *ACS Appl. Mater. Interfaces* **2018**, *10*, 21642.
[22] J. Zheng, P. Xiao, X. X. Le, W. Lu, P. The´ato, C. X. Ma, B. Y. Du, J. W. Zhang, Y. J. Huang, T. Chen, *J. Mater. Chem. C* **2018**, *6*, 1320.
[23] X. Peng, Y. Li, Q. Zhang, C. Shang, Q. W. Bai, H. L. Wang, *Adv. Funct. Mater.* **2016**, *26*, 4491.
[24] X. H. Zhou, T. Z. Li, J. H. Wang, F. Chen, D. Zhou, Q. Liu, B. J. Li, J. Y. Cheng, X. C. Zhou, B. Zheng, *ACS Appl. Mater. Interfaces* **2018**, *10*, 9077.
[25] S. W. Xiao, Y. Yang, M. Q. Zhong, H. Chen, Y. X. Zhang, J. T. Yang, J. Zheng, *ACS Appl. Mater. Interfaces* **2017**, *9*, 20843.
[26] Z. J. Wang, C. N. Zhu, W. Hong, Z. L. Wu, Q. Zheng, *Sci. Adv.* **2017**, *3*, 1700348.
[27] Z. Chen, D. H. Zhao, B. H. Liu, G. D. Nian, X. K. Li, J. Yin, S. X. Qu, W. Yang, *Adv. Funct. Mater.* **2019**, *29*, 1900971.
[28] C. X. Ma, T. F. Li, Q. Zhao, X. X. Yang, J. J. Wu, Y. W. Luo, T. Xie, *Adv. Mater.* **2014**, *26*, 5665.
[29] A. S. Gladman, E. A. Matsumoto, R. G. Nuzzo, L. Mahadevan, J. A. Lewis, *Nat. Mater.* **2016**, *15*, 413.
[30] L. M. Huang, R. Q. Jiang, J. J. Wu, J. Z. Song, H. Bai, B. G. Li, Q. Zhao, T. Xie, *Adv. Mater.* **2017**, *29*, 1605390.
[31] H. J. Lin, S. H. Ma, B. Yu, M. R. Cai, Z. J. Zheng, F. Zhou, W. M. Liu, *Chem. Mater.* **2019**, *31*, 4469.
[32] C. X. Ma, W. Lu, X. X. Yang, J. He, X. X. Le, L. Wang, J. W. Zhang, M. J. Serpe, Y. J. Huang, T. Chen, *Adv. Funct. Mater.* **2018**, *28*, 1704568.